Electronic Supplementary Material (ESI) for Journal of Materials Chemistry C.

Supporting Information

Bioinspired multi-functional wearable sensor with integrated light-induced actuator based on asymmetric graphene composite film

Ying Hu, Ke Qi, Longfei Chang, Jiaqin Liu, Lulu Yang, Majing Huang, Guan Wu,* Pin Lu, Wei Chen, and Yucheng Wu*

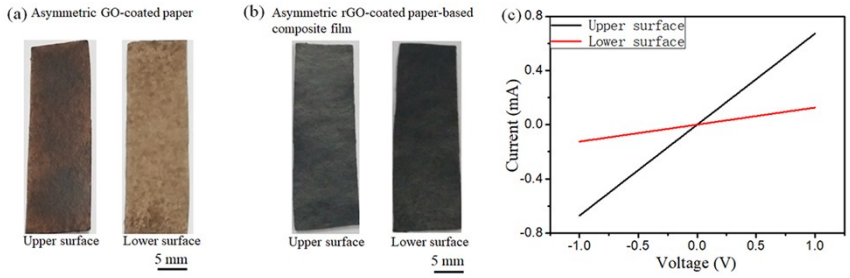

Figure S1. (a) Optical images of the upper (left image) and lower surface (right image) of the asymmetric GO-coated paper. (b) Optical image of the asymmetric rGO-coated paper-based composite film. The left one is the upper surface, and the right one is its lower surface. (c) I-V curves of the upper and lower surfaces of the rGO-coated paper-based composite film. The times of immersion of the above sample is 20.

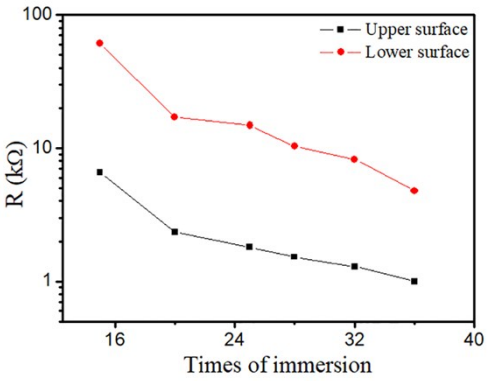

Figure S2. The upper surface and lower surface resistance of the rGO-coated paper-based composite film (35mm×10mm) with different immersion times.

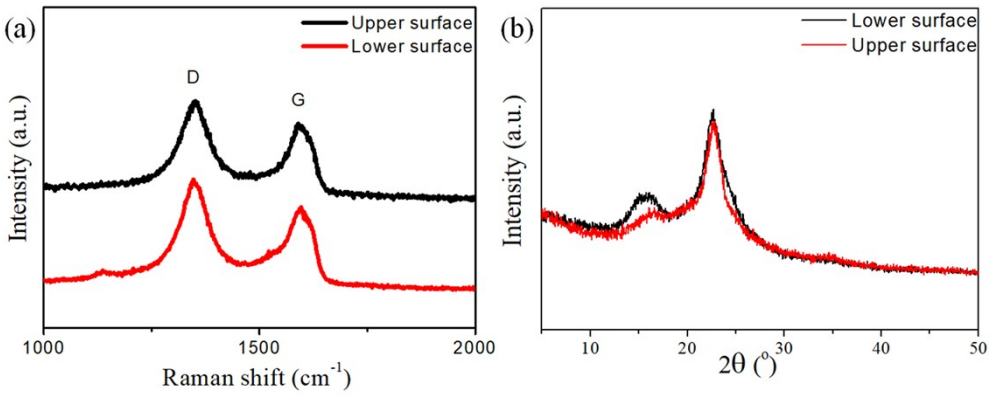

Figure S3. (a) Raman spectra of the upper surface (black curve) and lower surfaces (red curve) of rGO-coated paper-based composite film. The I_D/I_G difference in the upper surface and lower surface can be seen. (b) XRD patterns of the upper surface (black curve) and lower surface (red curve) of the rGO-coated paper-based composite film.

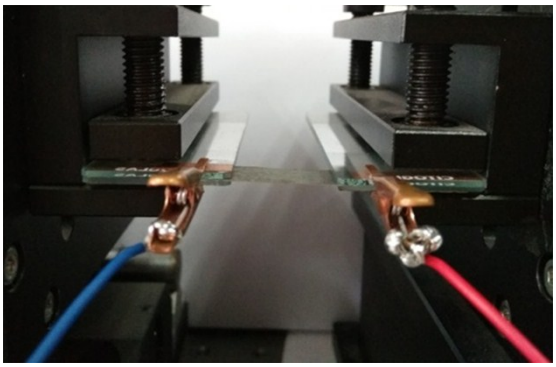

Figure S4. Optical image of the experimental setup used for measuring the strain sensing of the asymmetric rGO-coated paper-based composite film.

Calculation of the bending strain [1]

Assume that the composite film has a bending radius r, a chord length c, a central angle θ, and an arc length L. Therefore, their relationship can be expressed in Equation 1 and Equation 2:

$$\theta \times r = L \quad (1)$$

$$\sin(\theta/2) = c/2r \quad (2)$$

Then we can get the chord length as a function of radius, as shown in Equation 3:

$$c = 2r \times \sin(L/2r) \quad (3)$$

Assume that the bending central angle is θ_1, the correlation radius is r_1. In addition, θ_2 is related to r_2. Therefore, the compressive bending strain can be expressed in Equation 4:

$$\varepsilon = \Delta L/L = [\theta_2\times(r_2-z)-\theta_1\times(r_1-z)]/[\theta_1\times(r_1-z)] \quad (4)$$

where z is the distance away from the neutral layer of the rGO-paper substrate.

Because $r_1 >> z$, $\theta_1\times r_1 \approx \theta_2\times r_2$, the strain of Equation (4) can be further expressed in Equation 5 :

$$\varepsilon = z\times(\theta_1-\theta_2)/(\theta_1\times r) = z/r_1\times(1-\theta_2/\theta_1) = z/r_1\times(1-r_1/r_2) = z\times(1/r_1-1/r_2) \quad (5)$$

Since the original state of the composite film is flat, r_1 tends to infinity. Finally, the relationship between the compressive bending strain and the radius is given as an analysis in Equation 6:

$$\varepsilon = -z/r = -h/2r \quad (6)$$

where h is the thickness of the composite film. Simultaneously, the tensile bending strain calculate as in Equation 7

$$\varepsilon = h/2r \quad (7)$$

Here the thickness is 81μm, and the chord length decreased from 18 to 16mm and then returned to the original length.

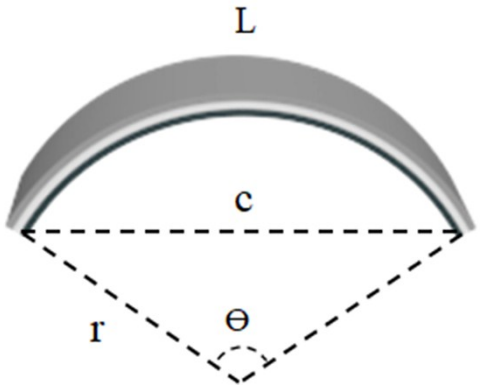

Figure S5. Schematic model image of the bending deformation of the sensor.

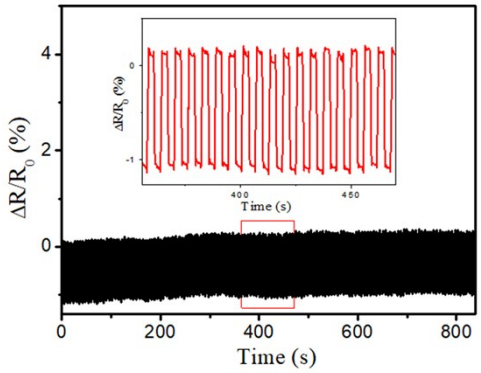

Figure S6. Relative resistance change of the sensor under cyclic bending-straightening deformation. The sensor still maintains good sensing performance after 300 cycles bending deformation.

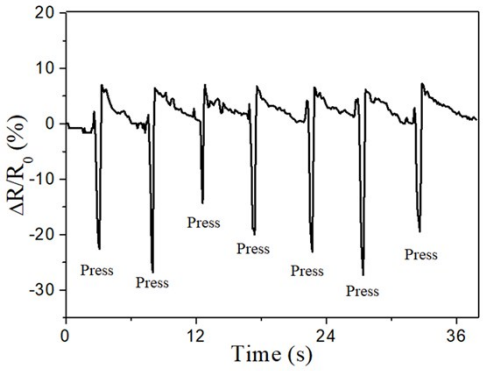

Figure S7. Resistance change of the sensor in response to the cyclic finger pressing.

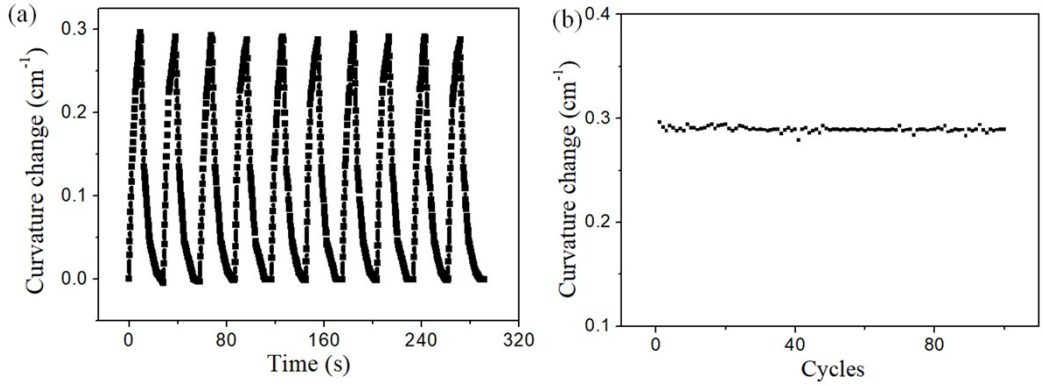

Figure S8. (a) Curvature change of the bilayer actuator upon cyclic light irradiation. (b) Long-term cyclic actuation of the bilayer actuator under light irradiation.

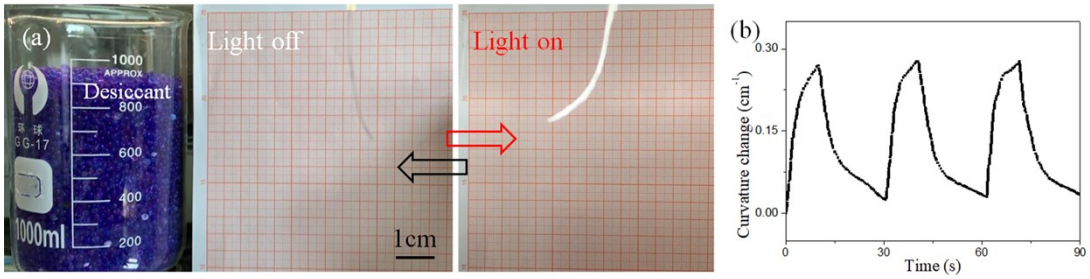

Figure S9. (a) Optical images of the light induced actuation in dry environment. The bilayer actuator is put inside a drying oven with the desiccant to keep the dry environment. (b) Cyclic light induced actuation of the bilayer actuator in dry environment.

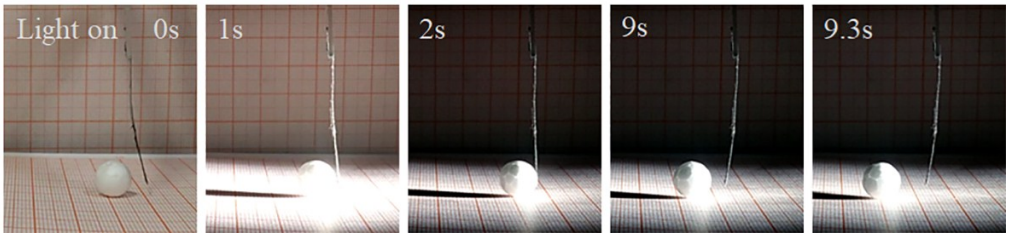

Figure S10. Optical images showing the bilayer actuator-based smart “leg” for kicking the ball away under the light irradiation.

Movie S1. Light-driven artificial flower based on bilayer actuators

Movie S2. The movement of light-driven crawling robot upon light irradiation

Movie S3. Smart leg for kicking the ball under light irradiation

References

1. X. Liao, Q. Liao, X. Yan, Q. Liang, H. Si, M. Li, H. Wu, S. Cao, Y. Zhang, *Adv. Funct. Mater.* **2015**, 25, 2395.